Canadian Science Publishing

ARTICLE

Impact of typhoon Matmo (2014) on the distribution of heavy metals in Quanzhou Bay[1]

Yunpeng Lin, Yunhai Li, Binxin Zheng, Xijie Yin, Liang Wang, Jia He, and Fangfang Shu

Abstract: The typhoon process has a significant influence on the distribution of heavy metals in sediments. Based on the heavy metal (V, Cr, Co, Ni, Cu, Zn, Pb, and Mn) contents in surface sediments collected under normal conditions and post-typhoon Matmo in Quanzhou Bay in 2014, the distributions, sources, and impacts of typhoon processes on heavy metals and pollution conditions were studied and discussed. The results showed that the heavy metals can be divided into two categories: Class I metals (Cu, Zn, Pb, and Mn) were mainly distributed in the estuary and significantly increased after the typhoon, and Class II metals (V, Cr, Co, and Ni) were distributed in the coastal intertidal zone and estuary and remained unchanged or decreased after the typhoon. The heavy metal assessment showed that heavy metal pollution in Quanzhou Bay was serious and tended to increase after the typhoon. The increased metal supply and enhanced riverine and tidal hydrodynamics after the typhoon may be the main factors influencing the variations in heavy metal content and distribution. This study provided a basis for the accurate evaluation and scientific management of heavy metal pollution caused by typhoon processes in Quanzhou Bay.

Key words: heavy metals, surface sediments, typhoon Matmo, Quanzhou Bay.

Introduction

With rapid socioeconomic development, a large amount of industrial and agricultural wastewater and domestic sewage produced by human activities has been discharged into the ocean through runoff or coastal outlets, causing serious heavy metal pollution in the estuary and coastal waters (Yu et al. 2016; Li et al. 2017). Heavy metal pollutants are a persistent potential hazard because they have toxic properties and are difficult to degrade, which can not only lead to ecological and environment deterioration, but also threaten human health by their cumulative transmission through the food chain (Doabi et al. 2018; Manoj et al. 2018). In recent years, scientists have carried out copious work on the sources, migration, flux, ecological hazards, and mechanisms of heavy metal pollutants and obtained a series of evidence providing a scientific basis for the abatement of heavy metal

Received 5 September 2018. Accepted 19 March 2019.

Y. Lin, B. Zheng, X. Yin, L. Wang, J. He, and F. Shu. Laboratory for Ocean and Coast Geology, Third Institute of Oceanography, Ministry of Natural Resources, Xiamen 361005, China.
Y. Li. Laboratory for Ocean and Coast Geology, Third Institute of Oceanography, Ministry of Natural Resources, Xiamen 361005, China; Laboratory for Marine Geology, Qingdao National Laboratory for Marine Science and Technology, Qingdao 266061, China.
Corresponding author: Yunhai Li (email: liyunhai@tio.org.cn).

[1]This paper is part of a Collection entitled "Coastal Environmental Changes under Increasing Anthropogenic Impacts".

pollution (Wang et al. 2003; Yan et al. 2009; Dou et al. 2013; Hu et al. 2013; Paula Filho et al. 2015). Among all the marine and surrounding coastal areas, the estuaries are a key area for studies of heavy metal pollution due to their unique sedimentary characteristics, dynamic environment, and close relationship with human activities (Radakovitch et al. 2008).

In an estuary, a large amount of the terrestrial material carried by a river settles, and the heavy metals attached to the surface of the fine particles are deposited and buried with sediments, thus making the estuarine sediments become a sink of heavy metal pollutants (Dou et al. 2013). Subsequently, with the influence of physical, chemical, and biological processes and human activities, this sink of heavy metals can be easily disturbed and transformed into a source for discharging pollutants to the open sea, resulting in the secondary pollution of heavy metals (Caplat et al. 2005; Anderson and Hayes 2015). The continuous conversion at the sediment–water interface with various external force disturbances constitutes the most basic cyclic process of heavy metals in an estuary (Martino et al. 2002; Song et al. 2011). Among disturbance factors, extreme weather on short-term scales, such as typhoons and winter storms, has extremely short-term effects on the water column and on sediment distribution for time periods of days to weeks (Pepper and Stone 2004; Wren and Leonard 2005), and it promotes the mixing of sediments and the heavy metals that are adsorbed to the fine-grain sediment (Pease et al. 2006). However, conducting relevant research on typhoon impacts is extremely difficult, and information is scarce due to the uncontrollable nature of the process and the difficulty of sampling. According to some rare studies, the strong dynamic processes accompanying typhoons, such as near-inertial internal waves caused by wind pulses during storm events (Puig et al. 2001), are likely to cause the resuspension, retransport, and redeposition of fine-grained particles in the marine environment (including estuaries, coasts, bays, and shelf areas) (Dickey et al. 1998; Wren and Leonard 2005; Xu et al. 2016), thus increasing the diffusion range of heavy metals adsorbed on the surface of fine-grained particles. Simultaneously, the heavy rainfall that occurs during typhoons increases the flow of rivers into the sea, as well as the discharge of various sewage outlets around the bay, leading to an increase in the flux of heavy metals entering the sea, and increasing the diffusion range of heavy metals (Li et al. 2010*a*, 2017). Therefore, the study of the typhoon process is particularly significant in terms of the distribution of heavy metals.

Quanzhou Bay, located on the southeast coast of Fujian Province and surrounded by developed light industry and aquaculture, is one of the most heavily polluted estuaries in Fujian Province (Yu et al. 2008, 2016; Hu et al. 2011*a*). Early studies showed that heavy metals in Quanzhou Bay mainly came from river input and that, due to the influence of small metal mines scattered along the coast of Fujian, Quanzhou Bay and its surrounding waters showed a unique characteristic of high Pb and Zn content (Xu et al. 1989). With the development of the economy, a large amount of industrial wastewater and domestic sewage is discharged directly or indirectly into the bay, which has become another major source of heavy metal pollutants in Quanzhou Bay (Gong et al. 2007; Hu et al. 2011*b*). Under riverine and tidal hydrodynamic influences, heavy metals are mainly distributed in the Jinjiang and Luoyangjiang estuaries and the coastal area of Quanzhou Bay (Yu et al. 2008, 2016; Li et al. 2010*b*). At the same time, the coastal area of Fujian Province, where Quanzhou Bay is located, is one of the areas that has been the most severely affected by typhoons in China, with an average of five to seven typhoons affecting the study area each year (Wang et al. 2008), making Quanzhou Bay an optimal natural laboratory for studying the impact of typhoons on the distribution of heavy metals in surface sediments. However, existing studies have focused on the source and distribution of heavy metals in the sediments of Quanzhou Bay under normal conditions, and only Li et al. (2010*a*) conducted research on the impact of the typhoon process on the distribution pattern of heavy metals in suspended particles. The results show that the content and distribution of heavy metals in suspended particles in a tidal cycle were significantly changed after a typhoon compared with normal conditions. The influence of the typhoon process on the distribution pattern and source input of heavy metals in surface sediments of Quanzhou Bay remains to be explored. Furthermore, studies on the influence of the typhoon process on the distribution of heavy metals in sediments were mainly concentrated on the continental shelf (Li et al. 2017), but small estuaries (or bays), such as Quanzhou Bay, which are an important component of the continental margin system, also need to be considered. Typhoon-related research carried out in small river estuaries is of great significance for understanding the response mechanism of the sedimentary dynamic environment of the continental margin system to the typhoon process.

To explore the impact of the typhoon process on the distribution of heavy metals in Quanzhou Bay, this study focused on the distribution characteristics of heavy metals, discussed the source of heavy metals, and evaluated the impact of the typhoon process based on the grain size measurement and heavy metal measurement data of surface sediment that were collected in normal conditions and post-typhoon Matmo. On this basis, we assessed heavy metal pollution and provided a scientific basis for the treatment of heavy metal pollution in Quanzhou Bay.

Background

Study area

The present study was carried out in Quanzhou Bay, which is a typical river-dominated bay (estuary) of China. The baymouth is open to the east, and at the top of the bay is the entrance to the Jinjiang River and the Luoyangjiang River. The total area of the bay is 136.42 km^2, of which the tidal flat area is 89.80 km^2. The main sediment in the Quanzhou Bay is derived from the input of the Jinjiang River, of which the annual runoff volume is 4.9×10^9 m^3/s and annual sediment flux is 2.54×10^6 t (Yang and Yin 2018). The Luoyangjiang River is a mountain stream river without flow into the sea due to a dam-building gate constructed in recent years, and its remaining river body is mainly seawater. The bay experiences semi-diurnal tide with a mean tidal range of 4.27 m, and the main type of tidal water movement is the stable reciprocating current. From above, the hydrodynamic processes of Quanzhou Bay are mainly controlled by river and tidal dynamics. Based on its regional geographical environment with hydrodynamic state, Quanzhou Bay can be divided into four areas from west to east: the estuary, the south channel, the north channel, and the bay mouth (Fig. 1*b*). The south channel is the ebb channel located in the south of Dazhui Island, while the north channel is the flood channel located in the north of Dazhui Island. They are independent at low tide and connected with each other at high tide. Furthermore, in the summer and autumn of each year, the strong winds and heavy rains of typhoon processes have become the main disastrous weather in Quanzhou Bay.

Typhoon Matmo

Typhoon Matmo, a severe tropical storm, made landfall in Fujian on 23 July 2014. The maximum wind force near the center was 11-grade (30 m/s), and the lowest pressure in the center was 980 hectopascals (http://agora.ex.nii.ac.jp/). The landfall location was approximately 100 km away from Quanzhou Bay, which was located in the 10-grade wind circle. Subsequently, typhoon Matmo passed through Fujian and Jiangxi Provinces, and it continued north to Shandong Province (Fig. 1*a*). Under the influence of Matmo, heavy rainstorms occurred in northwest and southeast Quanzhou. The inland rainfall was 150–250 mm, and the coastal area experienced 300–400 mm.

Fig. 1. (*a*) The track of typhoon Matmo (modified from the typhoon track data at http://agora.ex.nii.ac.jp/). The time point on the typhoon path represents the position of the typhoon center from 0000 (UTC) on 21 July 2014 to 1200 (UTC) on 24 July 2014. The black box is the research area of this paper. (*b*) The water depth of Quanzhou Bay. The hollow circle and red cross are the sampling stations, and the gray font shows the name of the tidal current zone.

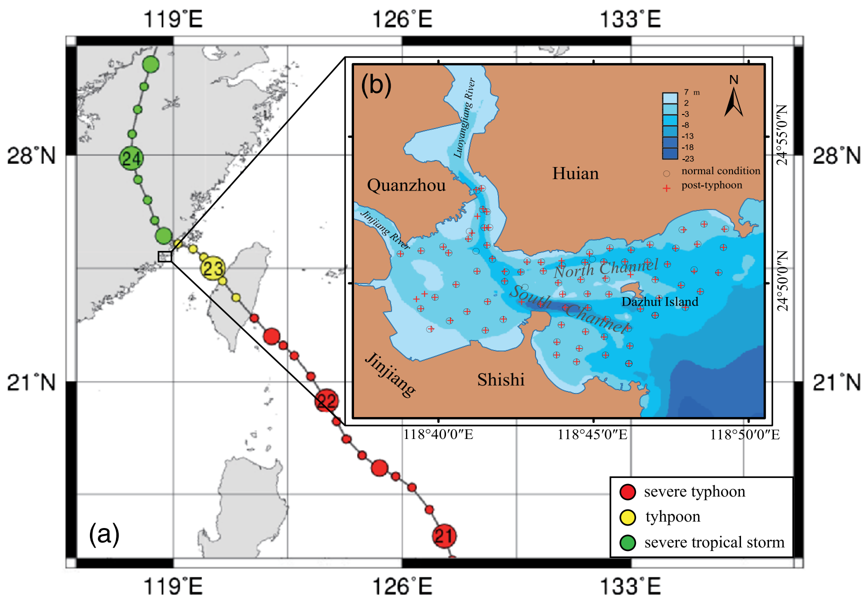

Materials and methods

Surveys and sampling

Based on the geographical location, climate characteristics, and influence of the typhoon, two surveys were conducted and 82 sampling stations were set in Quanzhou Bay (Fig. 1*b*). The first survey collected surface sediment samples 3–4 days after typhoon Matmo on 26–27 July 2014, and the second survey was conducted on 25–26 August 2014 in normal conditions without the typhoon influence. After each sample was obtained with a stainless steel sputum sampler, the uppermost 1~2 cm of sediment was collected in a sample bag with a wooden spoon, and it was then sealed and stored for laboratory analysis.

Grain-size and heavy metals measurement

The grain-size of the sediment was measured by a laser particle size analyzer (Mastersizer 2000, Malvern Instruments, Ltd., Malvern, UK). Approximately 0.5 g of fresh sediment was weighed. Next, 5 mL H_2O_2 was added to oxidize organic matter. Then, 5 mL HCl was added to dissolve shell debris after fully reacting; 5 mL sodium hexametaphosphate was then used to homogenize the sediment after acid washing, and it was then tested on the machine when particles were fully dispersed (Li et al. 2017). The measurement error of the instrument was within 3%. The grain-size fractions were <4 μm for clay, 4–63 μm for silt, and >63 μm for sand.

Due to the extremely low heavy metal content and the large measurement error in the sandy sediments, only fine-grained sediment samples were used for the determination of heavy metal contents (Tam and Wong 2000; Che et al. 2003). Closed-container dissolution was used to digest the sediments. Approximately 40 mg of dried and ground fine powders underwent digestion using 1 mL HF (GR, 40%) and 3 mL HNO_3 (GR/Merck, 65%) in Teflon containers for 12 h at 180 °C. The samples were then removed and placed on an electrothermal board to evaporate the HF. The residue was solubilized by 1 mL HNO_3 and 1 mL deionized water for 12 h at 150 °C. The V, Co, Ni, Cr, Cu, Zn, and Pb contents were measured by ICP-MS (iCAPQ, Thermo, Waltham, Mass.) and Mn and Al were measured by ICP-OES (iCAP7200, Thermo, Waltham, Mass.) after the extracted solution was diluted to a 40 mL volume with deionized water. One parallel sample was used for each of five samples, and two blank samples and two standard samples (GBW07316, marine sediment) were used for all samples. The error of the parallel sample, which was calculated by

$$\text{Error} = \frac{\text{STDEV}[\text{sample,parallel sample}]}{\text{AVERAGE}[\text{sample,parallel sample}]} \times 100\%$$

was less than 3%, and the test result of the standard sample falls within the standard range (the concentration of GBW07316).

The grain-size and heavy metal and Al content data of the sediment were measured in the Third Institute of Oceanography, Ministry of Natural Resources, China.

Statistical analysis methods

The data obtained were processed with statistical analyses including correlation analysis and principal component analysis (PCA) for heavy metals, Al, and grain-size, by SPSS 19.0 for Windows (SPSS Inc., Chicago, IL, USA). Pearson's correlation coefficient and a two-tailed test were used for correlation analysis. The significance level was set as $p = 0.05$ and the extremely significant difference level was set as $p = 0.01$.

PCA, a dimension reduction technique, is widely applied in environmental science studies and it is very effective in demonstrating the potential sources and spatial distribution of heavy metals (Gallego et al. 2002; Singh and Kumar 2017; Sun et al. 2018; Zhang et al. 2018). To better interpret the results of this study, the Varimax rotated factor matrix method, based on the orthogonal rotation criterion with Kaiser normalization, was applied to reduce the number of heavy metals that have high loadings on each factor and extract effective information from multidimensional data.

Heavy metals pollution assessment method

The multivariate potential ecological hazard index method, proposed by Hakanson (1980), is one of the most efficient and convenient heavy metal pollution assessment methods in the soil and sediment research (Maanan et al. 2015; Pejmana et al. 2015; Zhuang et al. 2018). This index is calculated as follows:

$$C_\mathrm{f}^i = \frac{C^i}{C_\mathrm{n}^i}$$

$$C_\mathrm{d} = \sum C_\mathrm{f}^i$$

$$E_\mathrm{m}^i = T_\mathrm{m}^i \times C_\mathrm{f}^i$$

$$\mathrm{RI} = k \sum E_\mathrm{m}^i$$

In the formulae, C_f^i is the pollution coefficient of a single element; C^i is the measured value of a heavy metal element; C_n^i is the background value of a heavy metal element (Liu 1995); C_d is the comprehensive pollution degree of sediment; E_m^i is the potential ecological risk coefficient of a single element; T_m^i is the toxicity coefficient of a heavy metal element (Liu 1995); and RI is the potential ecological risk index of heavy metals in sediment.

Results

Distribution and variation of grain-size in the sediments

The grain-size analysis results from Quanzhou Bay are shown in Table 1. The results indicate that the sediments in the study area are dominated by silt and clay, and the sand content is relatively low. According to the Shepard classification method (Shepard 1954), the sediments in Quanzhou Bay can be divided into sand (S), silty sand (TS), sandy silt (ST), silt (T), clay silt (YT), and sand–silt–clay (STY). Clay silt (YT) is the most common type of sediment in Quanzhou Bay, followed by sand (S). The distribution pattern of silt is similar to that of clay and is negatively correlated with sand (Fig. 2). Under normal conditions, the coarse-grained sediments are mainly distributed in the Jinjiang River estuary and around Dazhui Island (Fig. 2*c*-1). In addition, there are also high-sand-content areas in the northeastern part of the bay mouth. The areas with high values of silt are mainly concentrated in the coastal areas of Hui'an County and Jinjiang city and the central part of Quanzhou Bay (Fig. 2*b*-1). The clay fraction is principally distributed adjacent to the high-value areas of sand around the Jinjiang River estuary in Quanzhou Bay (Fig. 2*a*-1).

Compared to normal conditions, after the typhoon, the average content of the sand fraction decreased from 16.80% to 11.01%, and the distribution tended to be concentrated. The average content of the silt fraction increased from 59.34% to 64.59%, and the high-value zone expanded, while the average content of the clay fraction did not change significantly, from 23.86% to 24.40% (Table 1; Fig. 2). In the estuary of the Jinjiang River, the distribution of the sand fraction expanded, and a fine-grained sedimentary zone was formed in the southwestern waters of Dazhui Island. The content of silt increased approximately 5%–10% in the central part of Quanzhou Bay and the coastal waters of Hui'an, but the clay fraction did not change significantly (see Fig. 3 for grain size information).

Distribution and variation of heavy metals in the sediments

The content and distribution of heavy metals in Quanzhou Bay are shown in Table 1, and Figs. 4 and 5. Comparing the heavy metal contents measured after typhoon Matmo with those under normal conditions, the contents of V, Cr, and Ni decreased slightly (1%~2%), and the content of Co remained basically unchanged (only a 0.3% change), while those of Cu, Zn, Pb, and Mn increased significantly (5.1%~12.3%). The distribution patterns of heavy metals in Quanzhou Bay can be divided into two categories, which exhibit significant differences (Figs. 4 and 5).

V, Cr, Co, and Ni have similar distribution characteristics (Fig. 4). The high-concentration areas in normal conditions were mainly located in the Jinjiang River estuary, the intertidal zone of the coast, and the northeastern sea area. There was a band-shaped low-concentration area present along the south channel. In the post-typhoon survey, the high-concentration area in the Jinjiang estuary had decreased (approximately 14%–17%) and the range had been narrowed, while the high-concentration areas close to the south and northeastern coast showed an increased trend (Fig. 4*a*-2, 4*b*-2, and 4*c*-2). The band-shaped low concentration area of the south channel almost disappeared, and the concentration of heavy metals around Dazhui Island increased significantly (approximately 14%–20%).

Cu, Zn, Pb, and Mn have similar distribution characteristics (Fig. 5), and they show significant differences compared to the distribution patterns of V, Cr, Co, and Ni. The concentration of heavy metals decreased from the inner bay to the outer bay, and there was a distinctly high concentration area in the northwestern waters of Dazhui Island. In the post-typhoon survey, the heavy metal content in the estuaries of the Jinjiang River and Luoyangjiang River increased significantly (approximately 15%–25%), and a high-concentration area was formed off the southwest coast of Hui'an. Meanwhile, the concentration of heavy metals in the outer bay increased by approximately 10%–15%.

Table 1. The concentrations of clay (%), silt (%), sand (%), Al (%), and heavy metals (μg·g^{-1}).

	Clay	Silt	Sand	Al	V	Cr	Co	Ni	Cu	Zn	Pb	Mn
Normal conditions ($n = 59$)												
Mean	23.86	59.34	16.80	8.08	74.68	57.95	11.17	24.21	26.94	128.82	45.98	1101.00
Max	32.40	81.33	69.15	10.77	105.88	86.11	15.72	36.89	47.42	235.34	83.63	1855.29
Min	8.96	21.89	0.03	5.36	42.59	26.08	6.55	10.69	11.33	64.29	26.68	643.10
Post-typhoon ($n = 57$)												
Mean	24.40	64.59	11.01	8.37	73.25	56.79	11.20	23.91	29.54	135.38	51.66	1109.14
Max	32.85	79.81	70.09	10.78	112.66	94.39	16.48	39.82	63.80	274.45	107.98	2269.79
Min	7.06	22.85	0.71	5.87	36.55	19.07	5.88	7.68	10.04	64.67	29.50	512.90

Fig. 2. Distribution of clay (*a*), silt (*b*), and sand (*c*) in the sediment collected under normal (*a*-1, *b*-1, *c*-1) and post-typhoon (*a*-2, *b*-2, *c*-2) conditions.

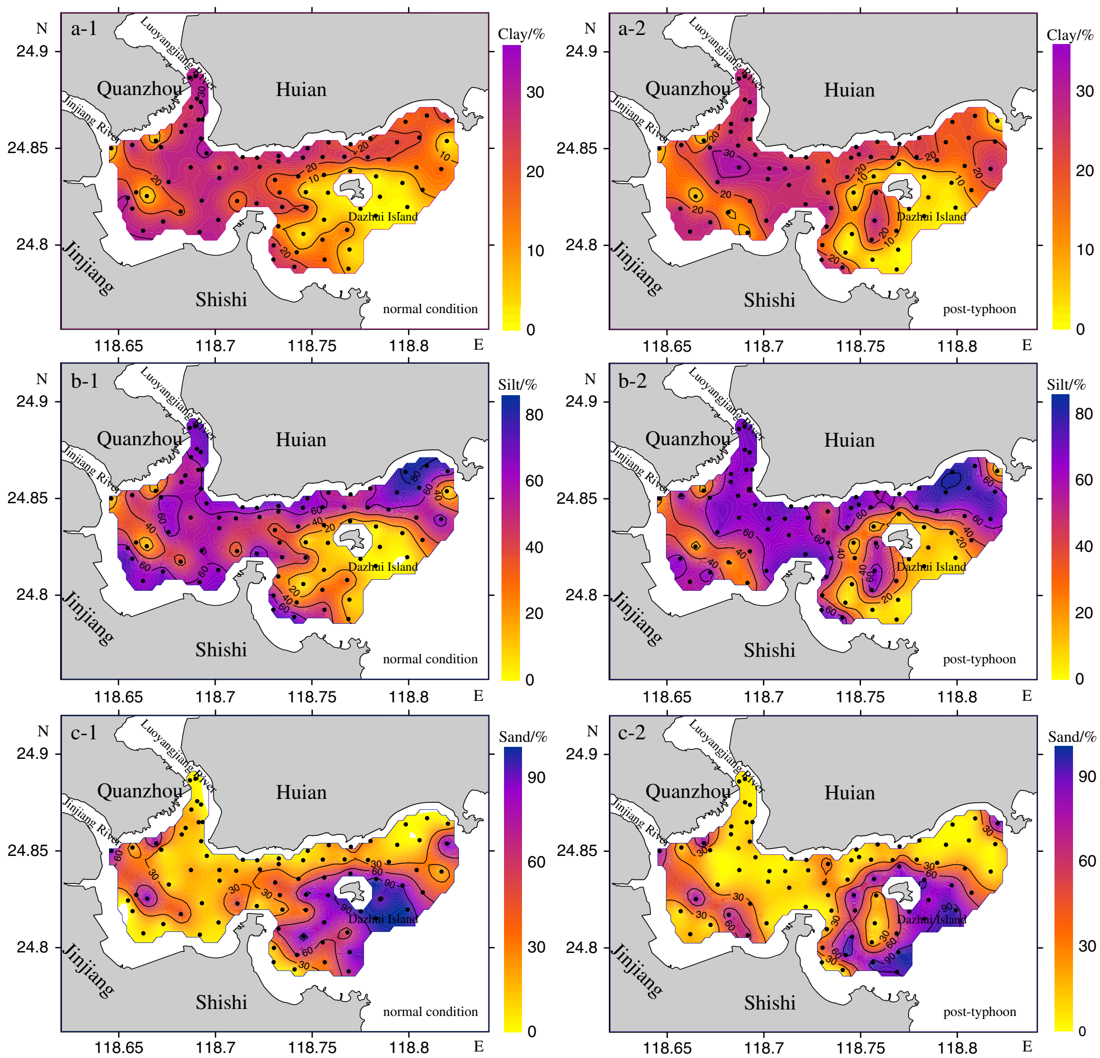

Fig. 3. The curve of standard deviation versus grain-size of the sediment in Quanzhou Bay.

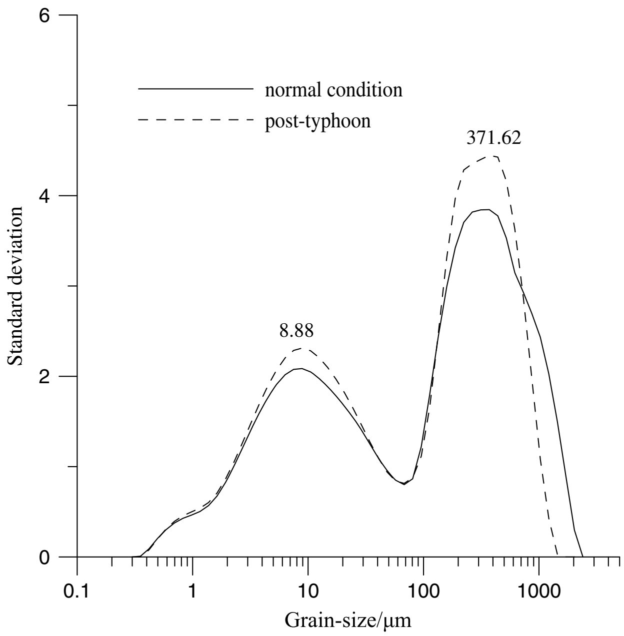

Relationships between grain-size and heavy metals in the sediments

The results of Pearson's correlation analysis (Table 2) showed that the concentrations of V, Cr, Co, and Ni were significantly correlated, and those of Cu, Zn, Pb, and Mn were significantly correlated, corresponding to two different distribution patterns of heavy metals and indicating that there may be two sources. From coarse particles (sand) to fine particles (clay), the correlation between the heavy metal content and the grain-size component content changed from a negative correlation to a positive correlation because the contact surface area (special surface area) increases with the sediment particles from large to small. As a result, the ability to adsorb heavy metals is gradually enhanced, and it is easy to attach inorganic colloids, such as Fe and Al oxides so that fine particles can adsorb more heavy metals (Tansel and Rafiuddin 2016). In the fine fraction, the concentrations of Cu, Zn, Pb, and Mn were positively correlated with the clay content, and the correlation with the silt content was not significant. However, V, Cr, Ni, and Co showed opposite results in that their concentrations were significantly positively correlated with silt content but showed no significant correlation with clay content (Table 2; Fig. 6).

Al is closely associated with the aluminosilicate fraction, which is the dominant metal-bearing phase of the sediment, as it can be used to determine whether the source of heavy metals is a natural source (Summers et al. 1996; Soto-Jiménez and Páez-Osuna 2001; Huang and Lin 2003). The correlation between heavy metals and Al elements (Table 2) revealed that Cu, Zn, Pb, and Mn were positively correlated with Al but V, Cr, Ni, and Al were not relevant, indicating that Cu, Zn, Pb, and Mn in the surface sediments of Quanzhou Bay were mainly derived from natural sources and that V, Cr, and Ni may mainly originate from anthropogenic sources. Co was positively correlated with Al in normal conditions, but the correlation was weaker than those of Cu, Zn, Pb, and Mn, and it was not related to Al in samples collected post-typhoon. The characteristics of Co suggest that it may have two sources, as a result of mixing natural sources with anthropogenic sources and that the anthropogenic source flux increased post-typhoon.

Fig. 4. Distribution of heavy metals V (*a*), Co (*b*), Cr (*c*), and Ni (*d*) under normal (*a*-1, *b*-1, *c*-1, *d*-1) and post-typhoon (*a*-2, *b*-2, *c*-2, *d*-2) conditions.

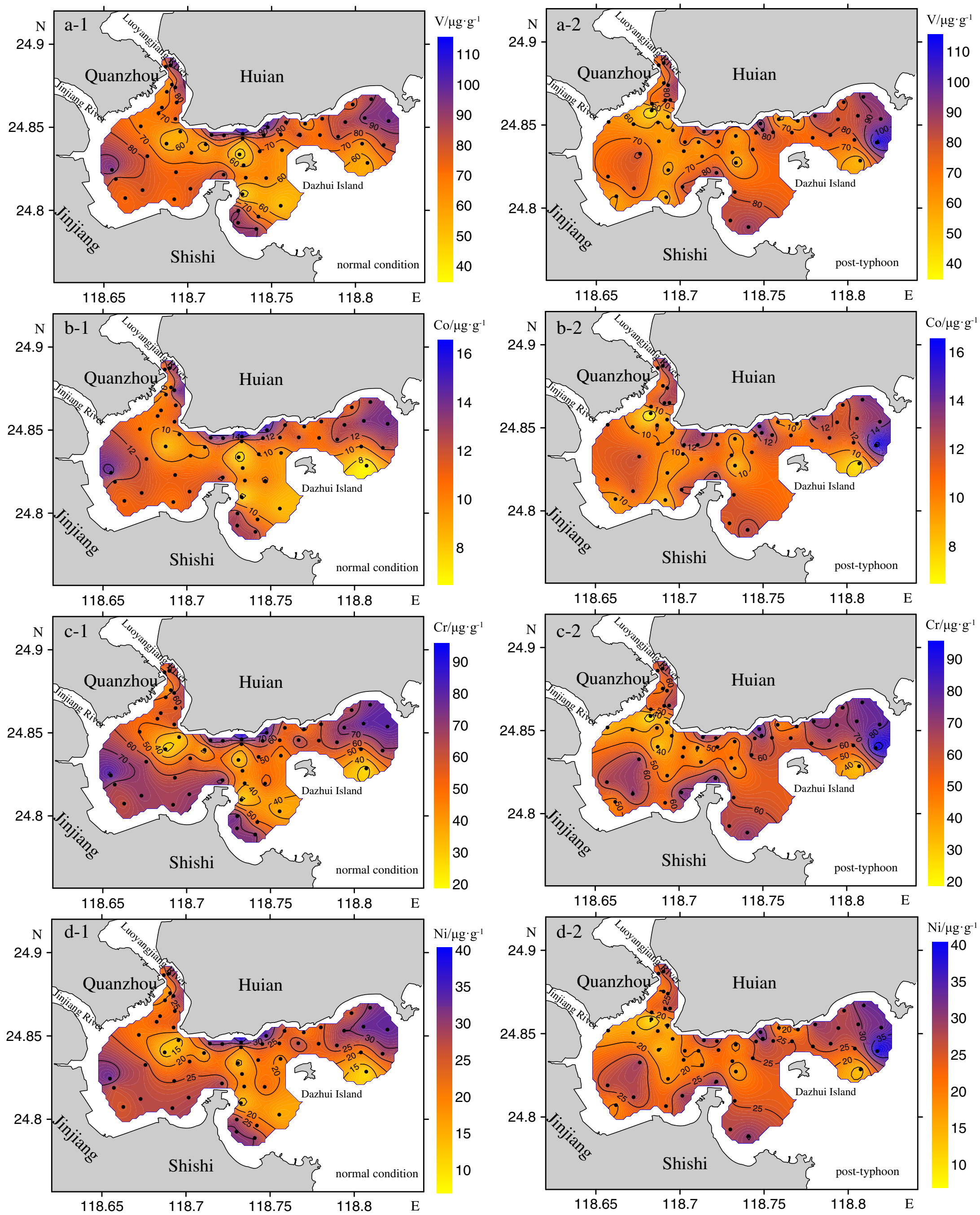

Fig. 5. Distribution of heavy metals Cu (*a*), Zn (*b*), Pb (*c*), and Mn (*d*) under normal (*a*-1, *b*-1, *c*-1, *d*-1) and post-typhoon (*a*-2, *b*-2, *c*-2, *d*-2) conditions.

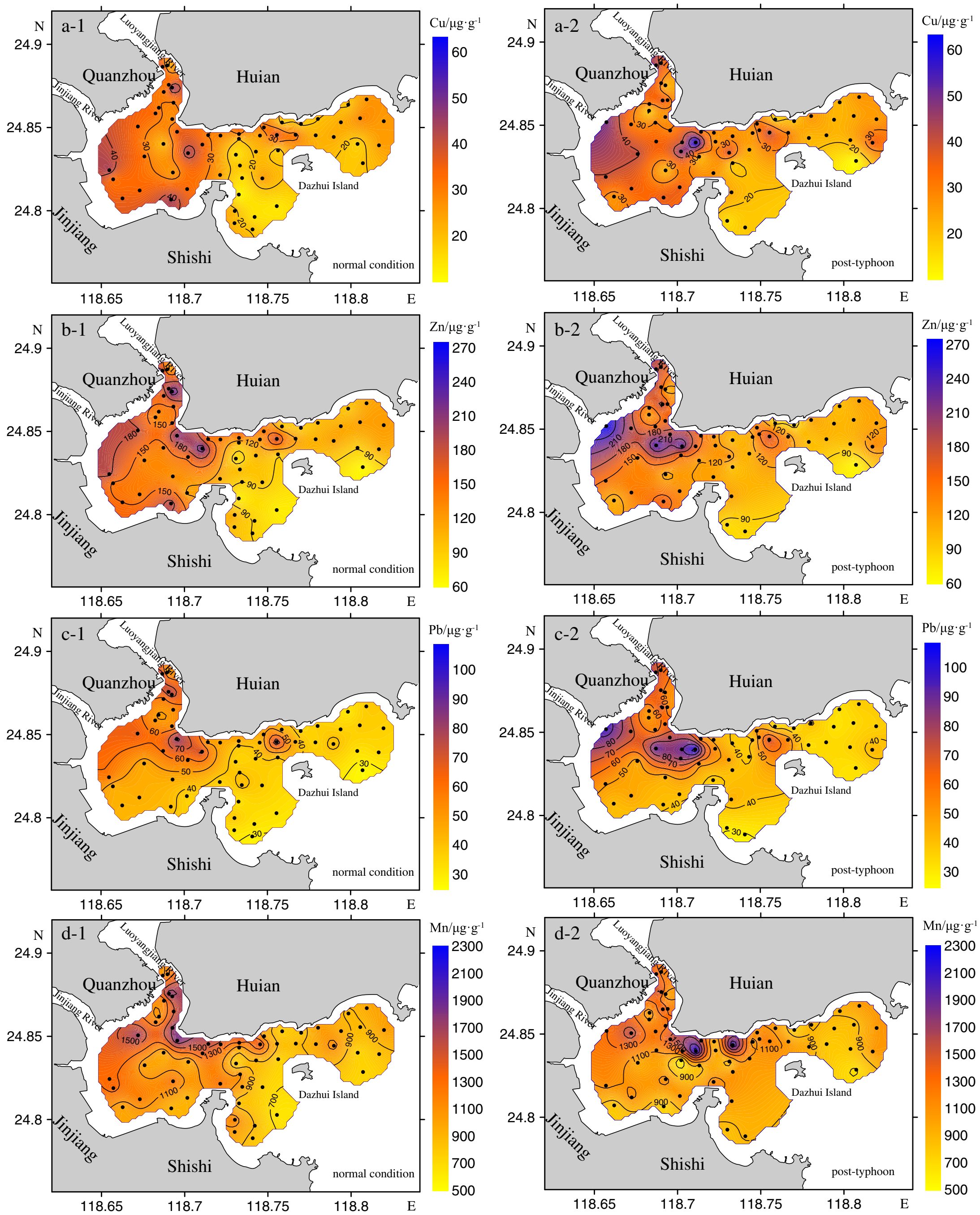

Table 2. Pearson's correlation coefficients for heavy metals, Al, clay, silt, and sand.

	V	Cr	Co	Ni	Cu	Zn	Pb	Mn	Al	Clay	Silt	Sand
Normal conditions (*n* = 59)												
V	1	—	—	—	—	—	—	—	—	—	—	—
Cr	0.939**	1	—	—	—	—	—	—	—	—	—	—
Co	0.965**	0.917**	1	—	—	—	—	—	—	—	—	—
Ni	0.958**	0.986**	0.945**	1	—	—	—	—	—	—	—	—
Cu	0.286*	0.320*	0.377**	0.322*	1	—	—	—	—	—	—	—
Zn	0.109	0.079	0.257	0.090	0.870**	1	—	—	—	—	—	—
Pb	−0.088	−0.199	0.062	−0.168	0.693**	0.891**	1	—	—	—	—	—
Mn	0.201	0.123	0.307*	0.119	0.474**	0.683**	0.642**	1	—	—	—	—
Al	0.247	0.230	0.308*	0.212	0.696**	0.748**	0.692**	0.689**	1	—	—	—
Clay	0.235	0.212	0.284*	0.204	0.666**	0.646**	0.588**	0.547**	0.705**	1	—	—
Silt	0.510**	0.508**	0.527**	0.486**	0.473**	0.398**	0.276*	0.389**	0.543**	0.749**	1	—
Sand	−0.455**	−0.446**	−0.483**	−0.427**	−0.566**	−0.504**	−0.394**	−0.466**	−0.631**	−0.690**	−0.778**	1
Post-typhoon (*n* = 57)												
V	1	—	—	—	—	—	—	—	—	—	—	—
Cr	0.929**	1	—	—	—	—	—	—	—	—	—	—
Co	0.938**	0.832**	1	—	—	—	—	—	—	—	—	—
Ni	0.952**	0.987**	0.881**	1	—	—	—	—	—	—	—	—
Cu	0.058	0.023	0.310*	0.077	1	—	—	—	—	—	—	—
Zn	−0.147	−0.280*	0.167	−0.200	0.816**	1	—	—	—	—	—	—
Pb	−0.240	−0.433**	0.033	−0.367**	0.755**	0.886**	1	—	—	—	—	—
Mn	−0.118	−0.204	0.113	−0.167	0.442**	0.643**	0.544**	1	—	—	—	—
Al	0.101	0.013	0.235	0.042	0.644**	0.540**	0.663**	0.410**	1	—	—	—
Clay	0.137	−0.031	0.251	0.000	0.398**	0.406**	0.546**	0.348**	0.627**	1	—	—
Silt	0.562**	0.489**	0.568**	0.472**	0.067	0.073	0.065	0.081	0.267	0.627**	1	—
Sand	−0.481**	−0.366**	−0.527**	−0.363**	−0.194	−0.201	−0.246	−0.187	−0.430**	−0.406**	−0.559**	1

**Correlation is significant at the 0.01 level (two-tailed).

*Correlation is significant at the 0.05 level (two-tailed).

Fig. 6. Relationship between clay and heavy metals V (*a*), Cr (*b*), Co (*c*), Ni (*d*), Cu (*e*), Zn (*f*), Pb (*g*), and Mn (*h*) in the seafloor sediment. V, Cr, Co, and Ni were not significantly correlated with clay content, while Cu, Zn, Pb, and Mn were significantly correlated with clay content. The slope of the fitting curve post-typhoon is obviously lower than that under normal conditions.

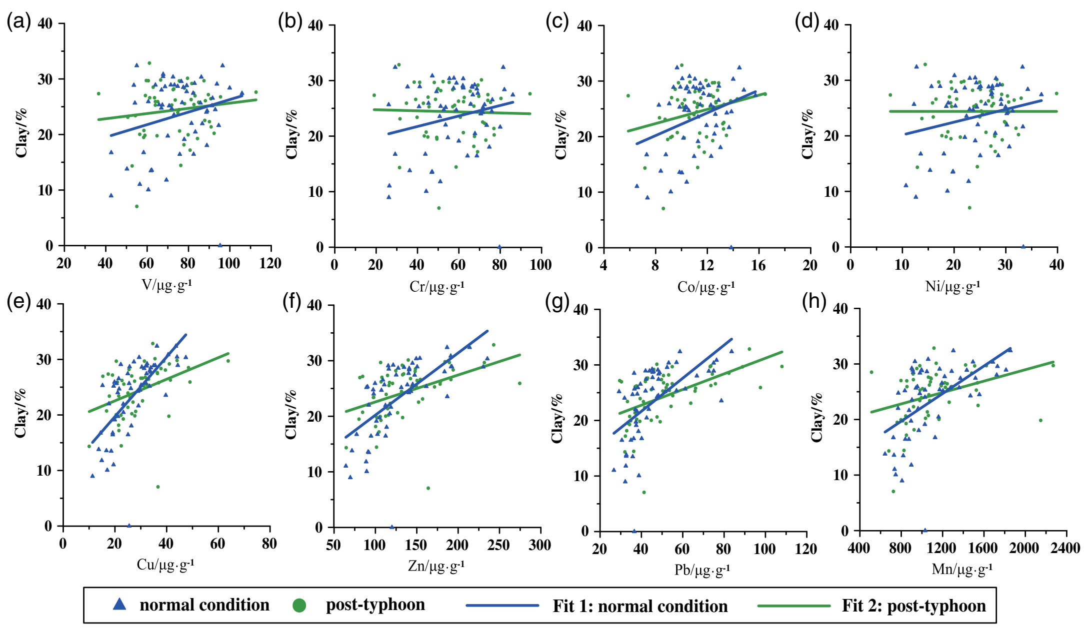

Identification of heavy metal sources using PCA

By performing PCA on the data, including the individual V, Cr, Co, Ni, Cu, Zn, Pb, Mn, and Al concentrations and sediment grain-size, the scree plots of eigenvalues and total variance explanation indicated that 89% of the data variance under normal conditions and 86% of the data variance post-typhoon could be explained by the first three components (Table 3).

Under normal conditions, PC1 accounted for 34.03% of the data variance and was distinguished by Cu, Zn, Pb, Mn, Al and clay with high positive loading, while the sand component had the highest negative loading. Combining with the distributions of Cu, Zn, Pb, and Mn (Fig. 5) and their high correlations with Al and clay, we consider that PC1 could be mainly attributed to river input. PC2 explained 33.84% of the data variance and was characterized by V, Cr, Co, and Ni with high positive loading, indicating a second source of heavy metals that was presumed to be coastal inputs based on their distribution characteristics (Fig. 4). PC3 elucidated 21.17% of the variance of the data, which were mainly characterized by positive loading of fine sediment and negative loading of coarse sediment; thus, it was considered to be a hydrodynamic effect.

After typhoon Matmo, the proportion of PC1 decreased to 31.56%, while PC2 increased to 33.48% and PC3 remained almost unchanged (21.04%). The loading of elements in principal components hardly changed. This indicates that typhoon Matmo did not change the sources of heavy metals in Quanzhou Bay.

Al and Mn are well known to be geogenic and are strongly correlated with Cu, Zn, and Pb but poorly correlated with V, Cr, Co, and Ni in PC1 (Tables 2 and 3), suggesting that Cu, Zn, Pb, and Mn may have a common source. There are significant correlations between PC1 and geological materials (i.e., Al and clay) while there was little correlation with anthropogenically induced trace elements. Therefore, we defined PC1 as a natural source. V, Cr, Co, and Ni are poorly correlated with Al, clay and the natural-source heavy metals (Cu, Zn, Pb, and Mn) in PC2 (Tables 2 and 3), so we assume that PC2 is mainly controlled by anthropogenic contributions. PC3 is only contributed by clay and silt with high negative loading of coarse sediment, so we attribute it to the impact of hydrodynamic force for heavy metals.

Heavy metal pollution assessment

The results of the multivariate potential ecological hazard index method are shown in Table 4. All metals exhibited moderate pollution except V, which exhibited low pollution, assessed by the criteria of Hakanson (1980). The potential risk index was low for all heavy metals, but the comprehensive pollution level was high; most of these values were moderate to high pollution, and all the heavy metals had similar contributions to the pollution. The degree of potential ecological risk assessment was minor. The high-pollution area was consistent with the high potential ecological risk area (Fig. 7), which was mainly concentrated in the estuary of Jinjiang River and Luoyangjiang River and coastal areas, consistent with the distribution of high-concentration areas of heavy metals and close to the source of heavy metals. Pollution tended to increase after the typhoon; however, the amount that heavy metal flux increased in the high-pollution area of the Jinjiang estuary was lower than dilution effects of runoff, and the pollution situation was alleviated.

Discussion

Differences in grain-size composition and its sedimentary (hydrodynamic) significance

The grain-size composition of sediments is a comprehensive reflection of factors like sediment sources and hydrodynamic processes (Whitmore et al. 2004; Bouchez et al. 2011). According to the results of grain-size analysis and previous studies (Wang 2007; Wang and Yu 2015), we deduce that the estuarine sediments supplied from the Jinjiang River were

Table 3. Rotated component matrix for different elements of sediment under normal conditions and post-typhoon (factor loadings exceeding 0.5 are indicated with bold fonts in rotated component).

	Normal conditions						Post-typhoon					
	Component matrix			Rotated component matrix			Component matrix			Rotated component matrix		
Element	PC1	PC2	PC3	PC1	PC2	PC3	PC1	PC2	PC3	PC1	PC2	PC3
V	0.659	0.711	0.145	0.055	**0.962**	0.180	−0.524	0.810	0.173	−0.075	**0.948**	0.236
Cr	0.632	0.748	0.105	−0.003	**0.965**	0.197	−0.647	0.707	0.230	−0.193	**0.960**	0.113
Co	0.728	0.613	0.228	0.199	**0.946**	0.154	−0.261	0.892	0.284	0.220	**0.918**	0.232
Ni	0.632	0.752	0.146	0.014	**0.980**	0.162	−0.600	0.739	0.284	−0.119	**0.982**	0.094
Cu	0.785	−0.313	0.232	**0.804**	0.249	0.245	0.662	0.452	0.462	**0.907**	0.182	−0.019
Zn	0.729	−0.559	0.302	**0.950**	0.044	0.174	0.836	0.306	0.301	**0.934**	−0.086	0.056
Pb	0.557	−0.728	0.248	**0.918**	−0.199	0.139	0.918	0.240	0.092	**0.894**	−0.264	0.201
Mn	0.650	−0.391	0.214	**0.756**	0.108	0.194	0.642	0.237	0.147	**0.684**	−0.099	0.112
Al	0.784	−0.393	0.066	**0.776**	0.138	0.391	0.613	0.520	0.009	**0.706**	0.069	0.380
Clay	0.791	−0.342	−0.358	**0.555**	0.064	**0.748**	0.514	0.572	−0.472	0.444	−0.041	**0.784**
Silt	0.806	0.085	−0.535	0.222	0.358	**0.875**	−0.093	0.780	−0.515	−0.006	0.414	**0.844**
Sand	−0.854	0.047	0.512	−0.344	−0.286	−0.891	−0.113	−0.806	0.566	−0.154	−0.304	−0.931

Note: Extraction method, PCA; rotation method: Varimax with Kaiser normalization.

Table 4. Heavy metals pollution assessment result.

	V	Cr	Co	Ni	Cu	Zn	Pb	Mn	C_d	RI
Normal conditions										
C	0.94	1.42	1.18	1.39	1.20	1.54	1.18	2.17	11.03	—
E	1.87	2.85	5.89	6.96	6.01	1.54	5.90	2.17	—	33.19
Post-typhoon										
C	0.92	1.40	1.18	1.37	1.32	1.62	1.32	2.19	11.32	—
E	1.84	2.79	5.91	6.87	6.59	1.62	6.62	2.19	—	34.43

Note: *C* is the pollution coefficient of a single element, *E* is the potential ecological risk coefficient of a single element, C_d is the comprehensive pollution degree of sediment, RI is the potential ecological risk index of heavy metals in sediment.

scoured by the strong tidal current (the current velocity is 0.2–1.4 m/s, as measured by the ADCP according to unpublished data), and fine sediments were transported and deposited on the shore or transported out of the water with the tidal currents, while coarser sediments remained in the estuary; most of these sediments belonged to river sediments that still comprised the coarse sediments of the river channel extending into the sea. Meanwhile, the coarse sediments from the river were blocked by Dazhui Island and formed a coarse-grained area that was also transformed by waves and tidal currents along the west coast of Dazhui Island (Fig. 2*c*-1). The strong hydrodynamic transportation of the south channel generated a coarse-grained concentrated area on the south of Dazhui Island. Northeast of Quanzhou Bay, high-sand-content areas may have been controlled by the surrounding topography, as the coarse-grained sediments in this area were mainly derived from the weathering and erosion of the surrounding sea headland, which were near-source accumulation. During the typhoon, the flow of Jinjiang River and the flux of sediments input into Quanzhou Bay increased due to heavy rainfall, and the hydrodynamic intensity of the estuary area was enhanced, leading to coarse sediments extending into the sea (Fig. 2*c*-2). At the same time, the strong dynamics of the typhoon hindered the sediment transportation along the south channel and established a fine-grained sedimentary area to the southwest of Dazhui Island.

Fig. 7. Distribution of C_d (*a*) and RI (*b*) under normal (*a*-1, *b*-1) and post-typhoon (*a*-2, *b*-2) conditions.

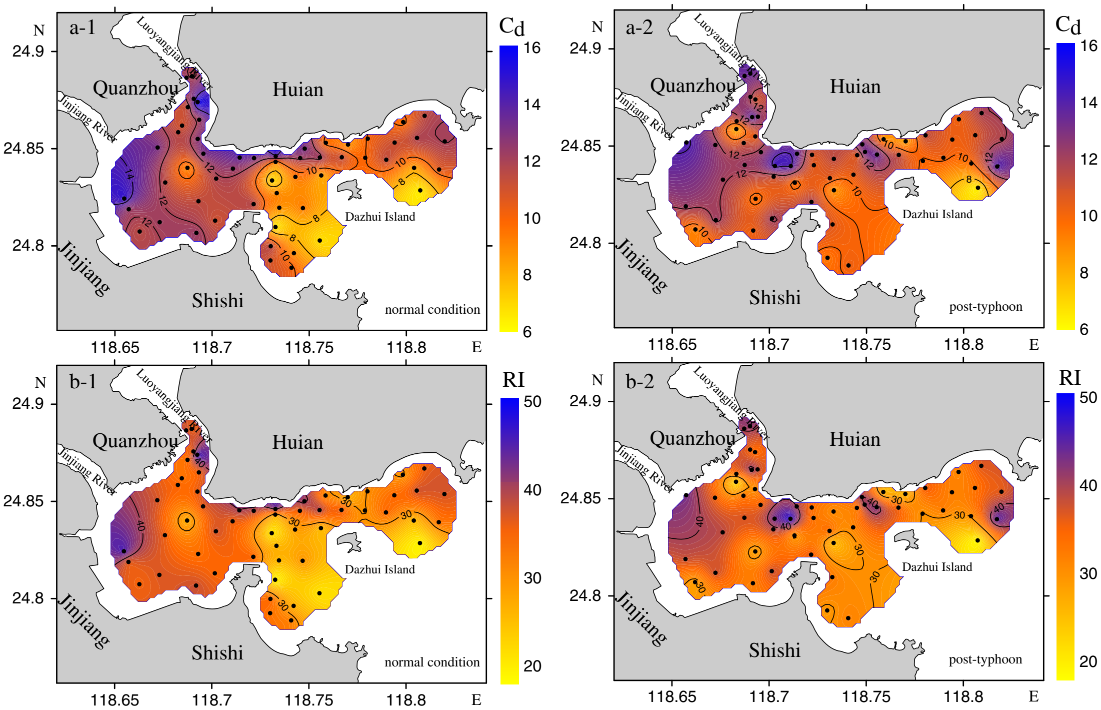

The sediment grain-size standard deviation curve, which mainly reflects the grain-size content variability of one sample group by each grain-size class, was used to extract the sensitive grain-size components that could indicate different sedimentary environments and dynamics (Liu et al. 2010; Fan et al. 2011). The sediment grain-size standard deviation curve is shown in Fig. 3 and indicates that the surface sediments of Quanzhou Bay have two standard deviation peaks (8.88 μm for silt and 371.62 μm for sand), reflecting that the sedimentation process was mainly affected by two different hydrodynamic forces, which may be riverine and tidal hydrodynamic forces. The riverine and tidal hydrodynamic forces in an estuary are the driving forces for the settlement and migration of heavy metals, and they affect the burial and diffusion of heavy metals (Pepper and Stone 2004). According to the curve (Fig. 3), the value of the standard deviation peaks increased, and the valley area remained unchanged post-typhoon, indicating that the two main hydrodynamic forces were significantly enhanced during typhoon conditions. With strong hydrodynamic forces, the fine sediments (mainly clay) were resuspended and migrated with the current flow, and the proportion of coarse particles increased in situ, eventually leading to the peak of the standard deviation. This resulted in the distribution of sand and silt being more concentrated due to their elutriation by the typhoon hydrodynamic forces. The elutriation of sand was significantly stronger than that of silt.

Sources and sinks of heavy metals and variable processes

The source of sediments is the factor that most directly affects the content and distribution of heavy metals (Huang and Lin 2003). The fine-grained components of sediments are the main storage medium for heavy metals in the process of transportation and deposition, and fine-grained sediments indirectly control the content and distribution of heavy metals by their content and distribution (Lin et al. 2002). According to the PCA results, the heavy metals Cu, Zn, Pb, and Mn mainly contributed to PC1, which was defined as a natural source, while V, Cr, Co, and Ni contributed to PC2 which was defined as an anthropogenic source. This means that the heavy metals in the Quanzhou Bay can be classified to two Classes by their sources supply.

Class I heavy metals (Cu, Zn, Pb, and Mn), which came from natural sources (mainly input from rivers), had similar distribution patterns (Fig. 5) and significantly correlated with each other (Table 2). They were mainly adsorbed on the surface of clay minerals with large specific surface areas or complexed with organic matter for transport and migration (Lin et al. 2002). Among them, Cu, Zn, and Pb originated from the weathering and erosion of basin rocks (Yu et al. 2016) and were then carried into the sea by Jinjiang River, thus forming a high-concentration area in the estuary that gradually decreased in concentration to the outer bay. Mn also had marine spontaneous sources in addition to the supply of weathering products carried by rivers (Hu et al. 2011*a*). In addition, the northern bank provided a certain contribution to such heavy metals, which may be derived from aquaculture. The coastal aquaculture industry in Hui'an County is well developed and contributed greatly to the heavy metals in the bay (Yu et al. 2008). However, in recent years, the aquaculture farms along the coastal areas of Hui'an County have been gradually closing with the increased attention that has been paid to environmental issues, and the impact of aquaculture on heavy metal pollution in the area has been decreasing.

Class II heavy metals (V, Cr, Ni, and Co) mainly came from anthropogenic inputs, including industrial and agricultural wastewater and stone processing (Hu et al. 2011*a*). They had similar distributions (Fig. 4) and high correlation coefficients (Table 3). Most metals in this class were deposited in the intertidal zone after being discharged from coastal areas (Yu et al. 2008) or were discharged into rivers in the middle and lower reaches of the river and then transported to the estuary (Gong et al. 2007). The heavy metals supplied from anthropogenic sources are transported and migrated over short distances and are less absorbed by clay minerals and organic matter, most of which are discharged directly into the sea from the coast and some of which are discharged into the river and transported to the bay by runoff. Therefore, the sediments in the intertidal zone of coastal areas and the estuary store high concentrations of heavy metals and have become the main sink for such heavy metals (Wang and Chen 2009). Jinjiang city and Shishi city on the south bank of Quanzhou Bay are the production bases for clothing, shoes, and hats, and the sewage produced by the printing, dyeing, textile, electroplating, and other industries is discharged into the bay through the sewage pipes of Jinjiang city and other areas in the south bank. Hui'an County, which is located on the north bank, is a famous stone production base, and a large amount of slurry processed by stone plate process is directly discharged to Quanzhou Bay from the north bank, resulting in a high concentration of silt and heavy metals in the coastal sediments of Hui'an.

During the typhoon, the flux of natural sources of heavy metals in the river increased with the increasing flow of runoff and flux of coastal sewage due to heavy rain, resulting in the high concentrations of heavy metals, such as Cu, Zn, Pb, and Mn in the estuary sediments. In contrast, the concentrations of anthropogenic heavy metals, such as V, Cr, Ni, and Co, decreased under the dilution from increased sediment flux, and the heavy metal content in the northeastern waters increased and spread to the south due to the increased coastal input flux and enhanced tidal dynamics. Furthermore, the heavy metals deposited in the sediments under normal conditions were resuspended and retransported under the strong typhoon force, which transformed the estuarine and near-shore intertidal sediments from a sink to a source for the secondary pollution of heavy metals and which changed the distribution pattern of heavy metals in the bay. Nearshore sediments that were rich in heavy metals, such as V, Cr, Ni, and Co, especially in the coastal area of Hui'an, were transported by coastal currents, resulting in a decrease in the concentration of heavy metals in the sediments of the region. However, Cu, Zn, Pb, and Mn were combined to form a high-concentration area under the dual effects of source input and dynamic disturbance in the estuary and at the intersection of the north channel and the south channel. Overall, the strong hydrodynamic forces during the typhoon enhanced the transport process of heavy metals, destroyed the original sink, established a new source–sink pattern, and expanded the scope of the sinks for the sedimentary storage of heavy metals.

Evolution of sedimentary process in Quanzhou Bay and impact of the typhoon on the distribution of heavy metals in the sediments

Under normal conditions (Fig. 8*a*), the migration and sedimentation processes of sediments in Quanzhou Bay are mainly controlled by the current. At high tide, the tidal current transported along the north channel to the inner bay encounters fresh water input from Jinjiang River at the estuary, forming a plume and a salinity wedge. A maximum turbidity zone develops in the front of the salinity wedge where the heavy metals settle into the sediment in large quantities with the river particles. At low tide, the mixed water is transported along the narrow south channel to the open sea. The coarser particles are deposited along the line to form a banded zone of low concentrations of heavy metals with enhanced hydrodynamic force. At the same time, coastal sewage outlets continue to discharge wastewater containing heavy metals, making the nearshore sediments rich in heavy metal pollutants. Hui'an Country, on the north shore, discharges a large amount of stone slurry, leading to a high level of silt and Class II heavy metal contents in coastal sediments.

During the typhoon (Fig. 8*b*), vertical mixing intensified and the estuary salinity wedge was weakened with the agitation of the strong hydrodynamic forces. At this point, Quanzhou Bay turned into a strong mixed estuary. Sediments that were originally deposited in the largest turbidity zone and in the intertidal zone of the estuary were resuspended and transported outward by the water flow, and deposited in areas with weak hydrodynamic forces, such as the cape bay. The flow of Jinjiang River increased, and a large amount of sediment was discharged into Quanzhou Bay, which expanded the distribution area of coarse sediments in the estuary. Meanwhile, fine sediments, such as silt, diffused and settled to the periphery. The increase in runoff flux with sediment and pollutants increased the concentration of heavy metal pollutants (Cu, Zn, Pb, and Mn) inputted into the sea by Jinjiang River and diluted the concentrations of heavy metal pollutants (V, Cr, Ni, and Co) that did not principally come from Jinjiang River. The effects of scouring and dilution from the large amount of rainwater input from the coastal sewage outlets caused the concentration of heavy metals in the coastal sediments to decrease, while the stone slurry input from the sewage outlets in the coastal areas of Hui'an, especially in the east, caused the concentration of silt and heavy metals (V, Cr, Co, and Ni) related to silt to increase.

Conclusion

Based on the measurements of heavy metals in the surface sediments acquired during two surveys (one under normal conditions and another after typhoon) in Quanzhou Bay, combined with sediment grain-size data, the impact of a typhoon on heavy metal distribution was determined and its mechanisms were discussed. The three main findings of this study, and their implications, are as follows:

1. Heavy metals in Quanzhou Bay can be divided into two categories: Class I metals (Cu, Zn, Pb, and Mn) mainly came from the natural weathering and erosion of parent rock with river input as the main supply, and their concentration decreased from the estuary to the sea.

Fig. 8. Conception evolution patterns of the typhoon impact on the sediments (including heavy metals) in Quanzhou Bay. The dark blue arrow indicates the moving direction of fresh water from the river, the purple arrow indicates the direction of the ocean's high salt water movement, the light blue arrow indicates the direction of the tidal current in the north and south channels of Quanzhou Bay, the yellow arrow indicates the path coastal sewage enters the sea, and the orange and black arrows indicate the paths of sediment transfer during typhoons: A, normal; and B, post-typhoon.

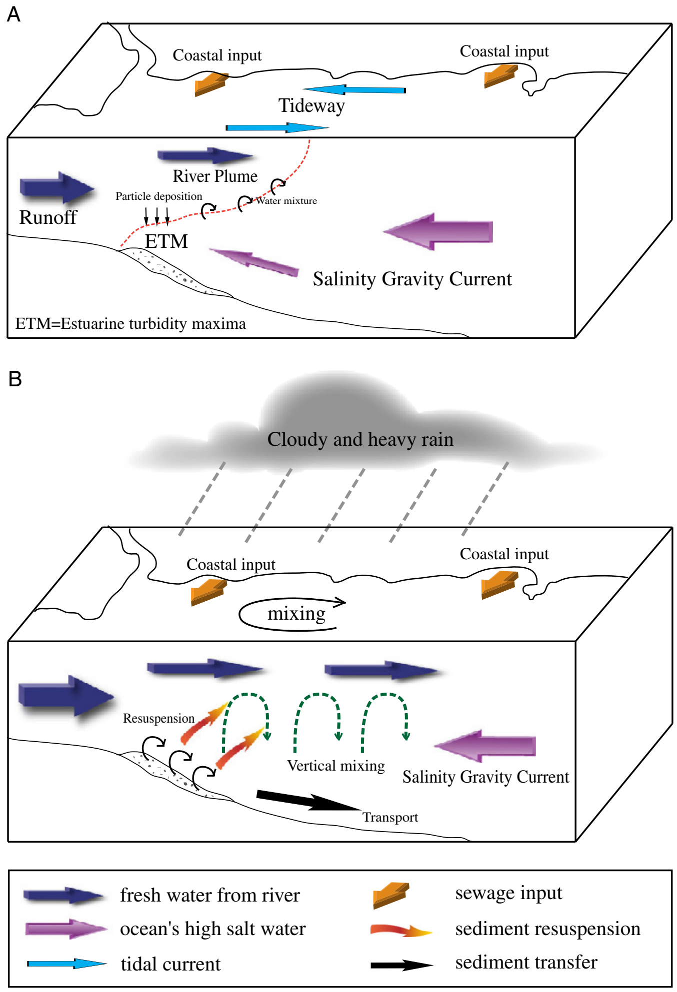

Class II metals (V, Cr, Co, and Ni) were mainly derived from artificial emissions and coastal input, and their high-concentration areas were distributed in estuaries and coastal areas.

2. The typhoon process had a significant impact on the source–sink pattern of heavy metals in Quanzhou Bay and had different effects on the two types of heavy metals. The flux of Class I heavy metals input into Jinjiang River during the typhoon increased significantly, forming a larger, high-concentration area in the estuary, and the original estuary sediment "sink" became the source of heavy metals transported into the sea. The input of Class II heavy metals decreased or remained unchanged during the typhoon, and the distributions were significantly affected by a strong dynamic process in which the original sediments with high heavy metal concentrations became the source of heavy metal redistribution in the bay.

3. The evaluation results of heavy metal pollution indicated that, except for V, which had low pollution levels, the elements in Quanzhou Bay were moderately polluted, and the pollution level of heavy metals was high. After the typhoon, pollution tended to increase and spread, which may have been caused by the larger metal supply and enhanced riverine and tidal hydrodynamics after the typhoon.

Acknowledgements

We thank all of the investigators for their help in collecting samples and data during the two surveys. This work was supported by the Scientific Research Foundation of the Third Institute of Oceanography, Ministry of Natural Resources (Nos. TIO2015014 and TIO2014016), the National Programme on Global Change and Air-Sea Interaction (No. GASI-GEOGE-03), and the National Science Foundation of China (NSFC, No. 41676028). This manuscript benefited from comments by an editor and two anonymous reviewers.

References

Anderson, R.F., and Hayes, C.T. 2015. Characterizing marine particles and their impact on biogeochemical cycles in the GEOTRACES program. Prog. Oceanogr. **133**: 1–5. doi: 10.1016/j.pocean.2014.11.010.

Bouchez, J., Gaillardet, J., France-Lanord, C., Maurice, L., and Dutra-Maia, P. 2011. Grain size control of river suspended sediment geochemistry: Clues from Amazon River depth profiles. Geochem. Geophys. Geosyst. **12**(3): Q03008. doi: 10.1029/2010GC003380.

Caplat, C., Texier, H., Barillier, D., and Lelievre, C. 2005. Heavy metals mobility in harbour contaminated sediments: The case of Port-en-Bessin. Mar. Pollut. Bull. **50**(5): 504–511. doi: 10.1016/j.marpolbul.2004.08.004. PMID: 15907492.

Che, Y., He, Q., and Lin, W.Q. 2003. The distributions of particulate heavy metals and its indication to the transfer of sediments in the Changjiang Estuary and Hangzhou Bay, China. Mar. Pollut. Bull. **46**: 123–131. doi: 10.1016/S0025-326X(02)00355-7. PMID: 12535978.

Dickey, T.D., Chang, G.C., Agrawal, Y.C., Williams, A.J., and Hill, P.S. 1998. Sediment resuspension in the wakes of Hurricanes Edouard and Hortense. Geophys. Res. Lett. **25**(18): 3533–3536. doi: 10.1029/98GL02635.

Doabi, S.A., Karami, M., Afyuni, M., and Yeganeh, M. 2018. Pollution and health risk assessment of heavy metals in agricultural soil, atmospheric dust and major food crops in Kermanshah province, Iran. Ecotoxicol. Environ. Saf. **163**: 153–164. doi: 10.1016/j.ecoenv.2018.07.057.

Dou, Y., Li, J., Zhao, J., Hu, B., and Yang, S. 2013. Distribution, enrichment and source of heavy metals in surface sediments of the eastern Beibu Bay, South China Sea. Mar. Pollut. Bull. **67**(1–2): 137–145. doi: 10.1016/j.marpolbul.2012.11.022. PMID: 23245460.

Fan, D.J., Qi, H.Y., Sun, X.X., Liu, Y., and Yang, Z.S. 2011. Annual lamination and its sedimentary implications in the Yangtze River delta inferred from High-resolution biogenic silica and sensitive grain-size records. Cont. Shelf Res. **31**(2): 129–137. doi: 10.1016/j.csr.2010.12.001.

Gallego, J.L.R., Ordóñez, A., and Loredo, J. 2002. Investigation of trace element sources from an industrialized area (Avilés, northern Spain) using multivariate statistical methods. Environ. Int. **27**: 589–596. doi: 10.1016/S0160-4120(01)00115-5. PMID: 11871393.

Gong, X., Qi, S., Lv, C., Su, Q., Wu, C., and Zhang, F. 2007. Concentration and distribution of heavy metals in surface sediment of Quanzhou Bay, Fujian Province. Environ. Sci. Technol. **30**(1): 27–28 [In Chinese with English abstract].

Hakanson, L. 1980. An ecological risk index for aquatic pollution control: A sedimentological approach. Water Res. **14**(8): 975–1001. doi: 10.1016/0043-1354(80)90143-8.

Hu, B., Li, J., Zhao, J., Yang, J., Bai, F., and Dou, Y. 2013. Heavy metal in surface sediments of the Liaodong Bay, Bohai Sea: Distribution, contamination, and sources. Environ. Monit. Assess. **185**(6): 5071–5083. doi: 10.1007/s10661-012-2926-0. PMID: 23064895.

Hu, G., Yu, R., Zhao, J., and Chen, L. 2011*a*. Distribution and enrichment of acid-leachable heavy metals in the intertidal sediments from Quanzhou Bay, southeast coast of China. Environ. Monit. Assess. **173**(1–4): 107–116. doi: 10.1007/s10661-010-1374-y.

Hu, G., Yu, R., Chen, L., Zhang, J., and Tu, X. 2011*b*. Evaluation of pollution of heavy metals in Luoyangjiang intertidal sediments, Quanzhou Bay. J. Mineral. Petrol. **31**(1): 109–115 [In Chinese with English abstract].

Huang, K.M., and Lin, S.W. 2003. Consequences and implication of heavy metal spatial variations in sediments of the Keelung River drainage basin, Taiwan. Chemosphere, **53**(9): 1113–1121. doi: 10.1016/S0045-6535(03)00592-7. PMID: 14512115.

Li, Y.H., Chen, J., Chen, J.N., Huang, C.B., Wang, A.J., and Li, D.Y. 2010*a*. Impact of typhoon "Fung-wong" on the distribution patterns of heavy metals in the Quanzhou Bay. Environ. Sci. **31**(6): 1450–1458. doi: 10.13227/j.hjkx.2010.06.024 [In Chinese with English abstract].

Li, Y.H., Chen, J., Huang, C.B., Wang, A.J., and Li, D.Y. 2010*b*. Distribution patterns of heavy metals in surface sediments of the Quanzhou Bay and environmental quality assessment. Environ. Sci. **31**(4): 931–939. doi: 10.13227/j.hjkx.2010.04.007 [In Chinese with English abstract].

Li, Y.H., Lin, Y.P., and Wang, L. 2017. Distribution of heavy metals in seafloor sediments on the East China Sea inner shelf: Seasonal variations and typhoon impact. Mar. Pollut. Bull. **129**(2): 534–544. doi: 10.1016/j.marpolbul.2017.10.027. PMID: 29108740.
Lin, S.W., Hsieh, I.J., Huang, K.M., and Wang, C.H. 2002. Influence of the Yangtze River and grain size on the spatial variations of heavy metals and organic carbon in the East China Sea continental shelf sediments. Chem. Geol. **182**: 377–394. doi: 10.1016/S0009-2541(01)00331-X.
Liu, S.F., Shi, X.F., Liu, Y.G., Qiao, S.Q., Yang, G., Fang, X.S., et al. 2010. Records of the East Asian winter monsoon from the mud area on the inner shelf of the East China Sea since the mid-Holocene. Chin. Sci. Bull. **55**(21): 2306–2314. doi: 10.1007/s11434-010-3215-3.
Liu, Y.Q. 1995. Study and application of the soil environmental background values in Fujian coastal zone. Mar. Environ. Sci. **14**(2): 68–73 [In Chinese with English abstract].
Maanan, M., Saddik, M., Maanan, M., Chaibi, M., Assobhei, O., and Zourarah, B. 2015. Environmental and ecological risk assessment of heavy metals in sediments of Nador lagoon, Morocco. Ecol. Indic. **48**: 616–626. doi: 10.1016/j.ecolind.2014.09.034.
Manoj, M.C., Thakur, B., Uddandam, P.R., and Prasad, V. 2018. Assessment of metal contamination in the sediments of Vembanad wetland system, from the urban city of Southwest India. Environ. Nanotechnol. Monit. Manage. **10**: 238–252. doi: 10.1016/j.enmm.2018.07.004.
Martino, M., Turner, A., Nimmo, M., and Millward, G.E. 2002. Resuspension, reactivity and recycling of trace metals in the Mersey Estuary, UK. Mar. Chem. **77**: 171–186. doi: 10.1016/S0304-4203(01)00086-X.
National Institute of Informatics (NII). 2014. Path way of typhoon. Available from http://agora.ex.nii.ac.jp/ [accessed 21–24 July 2014].
Paula Filho, F.J., Marins, R.V., De Lacerda, L.D., Aguiar, J.E., and Peres, T.F. 2015. Background values for evaluation of heavy metal contamination in sediments in the Parnaiba River Delta Estuary, NE/Brazil. Mar. Pollut. Bull. **91**(2): 424–428. doi: 10.1016/j.marpolbul.2014.08.022. PMID: 25284444.
Pease, P., Lecce, S., Gares, P., and Rigsby, C. 2006. Heavy metal concentrations in sediment deposits on the Tar River floodplain following Hurricane Floyd. Environ. Geol. **51**(7): 1103–1111. doi: 10.1007/s00254-006-0401-3.
Pejmana, A., Bidhendia, G.N., Ardestania, M., Saeedib, M., and Baghvanda, A. 2015. A new index for assessing heavy metals contamination in sediments: A case study. Ecol. Indic. **58**: 365–373. doi: 10.1016/j.ecolind.2015.06.012.
Pepper, D.A., and Stone, G.W. 2004. Hydrodynamic and sedimentary responses to two contrasting winter storms on the inner shelf of the northern Gulf of Mexico. Mar. Geol. **210**(1–4): 43–62. doi: 10.1016/j.margeo.2004.05.004.
Puig, P., Palanques, A., and Guillen, J. 2001. Near-bottom suspended sediment variability caused by storms and near-inertial internal waves on the Ebro mid continental shelf (NW Mediterranean). Mar. Geol. **178**: 81–93. doi: 10.1016/S0025-3227(01)00186-4.
Radakovitch, O., Roussiez, V., Ollivier, P., Ludwig, W., Grenz, C., and Probst, J.-L. 2008. Input of particulate heavy metals from rivers and associated sedimentary deposits on the Gulf of Lion continental shelf. Estuar. Coast. Shelf Sci. **77**(2): 285–295. doi: 10.1016/j.ecss.2007.09.028.
Shepard, F.P. 1954. Nomenclature based on sand-silt-clay ratios. J. Sediment. Res. **24**: 151–158. doi: 10.1306/D4269774-2B26-11D7-8648000102C1865D.
Singh, U.K., and Kumar, B. 2017. Pathways of heavy metals contamination and associated human health risk in Ajay River basin, India. Chemosphere, **174**: 183–199. doi: 10.1016/j.chemosphere.2017.01.103. PMID: 28161519.
Song, Y.X., Ji, J.F., Yang, Z.F., Yuan, X.Y., Mao, C.P., Frost, R.L., and Ayoko, G.A. 2011. Geochemical behavior assessment and apportionment of heavy metal contaminants in the bottom sediments of lower reach of Changjiang River. Catena, **85**(1): 73–81. doi: 10.1016/j.catena.2010.12.009.
Soto-Jiménez, M.F., and Páez-Osuna, F. 2001. Distribution and normalization of heavy metal concentrations in Mangrove and Lagoonal sediments from Mazatlán Harbor (SE Gulf of California). Estuar. Coast. Shelf Sci. **53**(3): 259–274. doi: 10.1006/ecss.2000.0814.
Summers, J.K., Wade, T.L., Engle, V.D., and Malaeb, Z.A. 1996. Normalization of metal concentrations in estuarine sediments from the Gulf of Mexico. Estuaries, **19**(3): 581–594. doi: 10.2307/1352519.
Sun, X., Fan, D., Liu, M., Tian, Y., Pang, Y., and Liao, H. 2018. Source identification, geochemical normalization and influence factors of heavy metals in Yangtze River Estuary sediment. Environ. Pollut. **241**: 938–949. doi: 10.1016/j.envpol.2018.05.050. PMID: 29929160.
Tam, N.F.Y., and Wong, Y.S. 2000. Spatial variation of heavy metals in surface sediments of Hong Kong mangrove swamps. Environ. Pollut. **110**: 195–205. doi: 10.1016/S0269-7491(99)00310-3. PMID: 15092834.
Tansel, B., and Rafiuddin, S. 2016. Heavy metal content in relation to particle size and organic content of surficial sediments in Miami River and transport potential. Int. J. Sediment. Res. **31**(4): 324–329. doi: 10.1016/j.ijsrc.2016.05.004.
Wang, A. 2007. Impact of human activities on depositional process of tidal flat in quanzhou bay of China. Chin. Geogr. Sci. **17**(3): 265–269. doi: 10.1007/s11769-007-0265-9.
Wang, A., Gao, S., Chen, J., and Li, D. 2008. Sediment dynamic responses of coastal salt marsh to typhoon "KAEMI" in Quanzhou Bay, Fujian Province, China. Chin. Sci. Bull. **54**(1): 120–130. doi: 10.1007/s11434-008-0365-7.
Wang, A.J., and Chen, J. 2009. Spatial variations in depth-distribution of trace metals in coastal wetland sediments from Quanzhou Bay, Fujian Province, China. Chin. Geogr. Sci. **19**(1): 83–88. doi: 10.1007/s11769-009-0083-3.
Wang, S.X., Zhang, S.Z., and Shan, X.Q. 2003. Fractionation of heavy metals in different particle-size sediments and its relationship with heavy metal pollution. Bull. Environ. Contam. Toxicol. **71**: 873–880. doi: 10.1007/s00128-003-0223-x.

Wang, Z.D., and Yu, D.S. 2015. Characteristics of grain size in surface sediments of Quanzhou Bay. J. Appl. Oceanogr. **34**(3): 326–333. doi: 10.3969/J.ISSN.2095-4972.2015.04.016 [In Chinese with English abstract].

Whitmore, G.P., Crook, K.A.W., and Johnson, D.P. 2004. Grain size control of mineralogy and geochemistry in modern river sediment, New Guinea collision, Papua New Guinea. Sediment. Geol. **171**(1–4): 129–157. doi: 10.1016/j.sedgeo.2004.03.011.

Wren, P.A., and Leonard, L.A. 2005. Sediment transport on the mid-continental shelf in Onslow Bay, North Carolina during Hurricane Isabel. Estuar. Coast. Shelf Sci. **63**(1–2): 43–56. doi: 10.1016/j.ecss.2004.10.018.

Xu, A., Luo, B., and Chen, S. 1989. Geochemistry of heavy metals in surface sediment of Quanzhou Bay, Fujian. J. Oceanogr. Taiwan Strait, **8**(1): 383–388 [In Chinese with English abstract].

Xu, K.H., Mickey, R.C., Chen, Q., Harris, C.K., Hetland, R.D., Hu, K., and Wang, J.Z. 2016. Shelf sediment transport during hurricanes Katrina and Rita. Comput. Geosci. **90**: 24–39. doi: 10.1016/j.cageo.2015.10.009.

Yan, C., Li, Q., Zhang, X., and Li, G. 2009. Mobility and ecological risk assessment of heavy metals in surface sediments of Xiamen Bay and its adjacent areas, China. Environ. Earth Sci. **60**(7): 1469–1479. doi: 10.1007/s12665-009-0282-3.

Yang, S., and Yin, P. 2018. Sediment source-to-sink processes of small mountainous rivers under the impacts of natural environmental changes and human activities. Mar. Geol. Quat. Geol. **38**(1): 1–10. doi: 10.16562/j.cnki.0256-1492.2018.01.001 [In Chinese with English abstract].

Yu, R., Yuan, X., Zhao, Y.H., Hu, G.R., and Tu, X.L. 2008. Heavy metal pollution in intertidal sediments from Quanzhou Bay, China. J. Environ. Sci. **20**(6): 664–669. doi: 10.1016/S1001-0742(08)62110-5. PMID: 18763559.

Yu, R., Zhang, W., Hu, G., Lin, C., and Yang, Q. 2016. Heavy metal pollution and Pb isotopic tracing in the intertidal surface sediments of Quanzhou Bay, southeast coast of China. Mar. Pollut. Bull. **105**(1): 416–421. doi: 10.1016/j.marpolbul.2016.01.047. PMID: 26849914.

Zhang, X., Wei, S., Sun, Q., Wadood, S.A., and Guo, B. 2018. Source identification and spatial distribution of arsenic and heavy metals in agricultural soil around hunan industrial estate by positive matrix factorization model, principle components analysis and geo statistical analysis. Ecotoxicol. Environ. Saf. **159**: 354–362. doi: 10.1016/j.ecoenv.2018.04.072.

Zhuang, W., Wang, Q., Tang, L., Liu, J., Yue, W., Liu, Y., et al. 2018. A new ecological risk assessment index for metal elements in sediments based on receptor model, speciation, and toxicity coefficient by taking the Nansihu Lake as an example. Ecol. Indic. **89**: 725–737. doi: 10.1016/j.ecolind.2018.02.033.